Journal of Biomolecular NMR, **18:** 49–63, 2000.
KLUWER/ESCOM

Simulations of NMR pulse sequences during equilibrium and non-equilibrium chemical exchange

Magnus Helgstrand, Torleif Härd & Peter Allard*
Department of Biotechnology, Center for Structural Biochemistry, The Royal Institute of Technology (KTH), Novum, S-141 57 Huddinge, Sweden

Received 27 April 2000; Accepted 30 June 2000

Key words: average Liouvillian theory, chemical exchange, homogeneous master equation, McConnell equations, NMR simulations

Abstract

The McConnell equations combine the differential equations for a simple two-state chemical exchange process with the Bloch differential equations for a classical description of the behavior of nuclear spins in a magnetic field. This equation system provides a useful starting point for the analysis of slow, intermediate and fast chemical exchange studied using a variety of NMR experiments. The McConnell equations are in the mathematical form of an inhomogeneous system of first-order differential equations. Here we rewrite the McConnell equations in a homogeneous form in order to facilitate fast and simple numerical calculation of the solution to the equation system. The McConnell equations can only treat equilibrium chemical exchange. We therefore also present a homogeneous equation system that can handle both equilibrium and non-equilibrium chemical processes correctly, as long as the kinetics is of first-order. Finally, the same method of rewriting the inhomogeneous form of the McConnell equations into a homogeneous form is applied to a quantum mechanical treatment of a spin system in chemical exchange. In order to illustrate the homogeneous McConnell equations, we have simulated pulse sequences useful for measuring exchange rates in slow, intermediate and fast chemical exchange processes. A stopped-flow NMR experiment was simulated using the equations for non-equilibrium chemical exchange. The quantum mechanical treatment was tested by the simulation of a sensitivity enhanced ^{15}N-HSQC with pulsed field gradients during slow chemical exchange and by the simulation of the transfer efficiency of a two-dimensional heteronuclear cross-polarization based experiment as a function of both chemical shift difference and exchange rate constants.

Introduction

Nuclear magnetic resonance has become one of the standard techniques for the study of molecular dynamics and chemical kinetics and the theory is well established (Kaplan and Fraenkel; 1980, Kühne et al., 1979; Wennerström, 1972; Jeener, 1982; Kaplan, 1958; McConnell, 1958; Gutowsky et al., 1953; Binsch, 1969). The exchange of a nucleus between environments due to conformational transitions or chemical reactions can be monitored using a number of different NMR methods.

*To whom correspondence should be addressed. E-mail: peter@csb.ki.se

In order to discuss chemical exchange as studied by NMR it is useful to examine the case in which a nucleus exchanges with a rate constant k between two sites with different offset frequencies, Ω_I and Ω_S. Three different situations can then be distinguished (McLaughlin and Leigh, 1973). If the exchange rate is slow compared to the frequency difference, $k \ll |\Omega_I - \Omega_S|$, two distinct resonance lines are observed at Ω_I and Ω_S. Only a single resonance line is observed at the population weighted average chemical shift if the exchange rate is fast compared the chemical shift difference, $k \gg |\Omega_I - \Omega_S|$. The third possibility is the intermediate chemical exchange or coalescence case, which occurs when the exchange rate is similar in magnitude to the frequency difference, $k \approx$

$|\Omega_I - \Omega_S|$. Coalescence is easily identified by excessive line broadening that might make the resonance disappear into the background noise.

Different NMR techniques are applied in order to study chemical exchange occurring at different time scales. Slow exchange reactions are usually studied using methods based on longitudinal magnetization such as saturation transfer (Forsén and Hoffman, 1963) or selective inversion recovery. Line-shape analysis is a powerful technique when the system is in the intermediate exchange regime (Gutowsky et al., 1953; Kaplan, 1958; McConnell, 1958; Binsch, 1969). For rapid exchange the measurement of T_2 or $T_{1\rho}$ as a function of effective RF field strength, either on-resonance (Bloom et al., 1965, Deverell et al., 1970) or off-resonance (Akke and Palmer, 1996), can be used in order to determine the exchange rate constant.

The Bloch equations (Bloch, 1946) modified for the effects of chemical exchange, the McConnell equations (McConnell, 1958), are a convenient theoretical starting point for studies of chemical exchange whatever exchange regime or experimental method is used. The McConnell equations are in the form of a system of inhomogeneous first-order differential equations. The complications caused by the inhomogeneous form can be solved by separating the equation system into a transverse part and a longitudinal part (Cavanagh et al., 1996; Ernst et al., 1987). This can only be done if the transverse components of magnetization are not allowed to interchange with the longitudinal magnetization. The transverse part of the McConnell equations is immediately homogeneous and form the basis for line-shape calculations (McConnell, 1958). The longitudinal part can be made homogeneous with the help of a simple substitution if the system is in chemical equilibrium. These methods of treating the inhomogeneous differential equation system are obviously not complete solutions to the problem since the effect of pulse sequences can not be simulated when transverse and longitudinal magnetization are not allowed to interchange.

The McConnell system of equations can however be rewritten in a homogeneous form without introducing any approximations. With this new system of equations complete pulse sequences can be simulated taking into account chemical shifts, RF fields, relaxation and chemical exchange. The equation system is easily extended to larger spin systems.

The McConnell equations can not be used in order to simulate non-equilibrium chemical exchange since the equilibrium magnetization under such circumstances is time dependent. In this paper we show an equation system that can treat both equilibrium and non-equilibrium chemical exchange, as long as the kinetics is of first order. This method of handling first-order kinetics can be used together with both classical mechanics and quantum mechanics.

A quantum mechanical treatment is necessary whenever the effects of scalar couplings can not be ignored. The quantum mechanical description of spin dynamics can be combined with chemical exchange in the same way as the McConnell equations combine a classical description of spin dynamics with chemical exchange. The same method of rewriting the inhomogeneous system of equations into a homogeneous system used for the McConnell equation can be applied to the quantum mechanical description.

Theory

We will first describe the theory for a simple two-site first-order chemical reaction in matrix form and discuss how it can be extended to a larger number of coupled first-order reactions. We will then discuss the Bloch equations in matrix form and show how the McConnell equations can be derived using a product space of chemical configuration space and the magnetization space. We will show how the McConnell equations can be made homogeneous using two different but similar methods. The first method can be applied to systems in chemical equilibrium while the other method is also applicable for non-equilibrium systems. Finally, we discuss how a complete quantum mechanical theory for a heteronuclear two-spin system in chemical exchange can be obtained using the same method as described for classical mechanics.

Chemical exchange

A simple first-order chemical exchange reaction with two components can be described according to (Cavanagh et al., 1996, Ernst et al., 1987)

$$[I] \underset{k_{SI}}{\overset{k_{IS}}{\longleftrightarrow}} [S], \tag{1}$$

where k_{IS} and k_{SI} are the exchange rate constants for the forward and reverse reactions, respectively. The differential equation system for this chemical ex-

change is easily set up according to the chemical reaction rate law

$$\begin{aligned}\frac{\mathrm{d}}{\mathrm{d}t}[I] &= -k_{IS}[I] + k_{SI}[S],\\ \frac{\mathrm{d}}{\mathrm{d}t}[S] &= +k_{IS}[I] - k_{SI}[S],\end{aligned} \tag{2}$$

which can be written in matrix form as

$$\frac{\mathrm{d}}{\mathrm{d}t}\begin{bmatrix}[I]\\ [S]\end{bmatrix} = \begin{bmatrix}-k_{IS} & k_{SI}\\ k_{IS} & -k_{SI}\end{bmatrix}\begin{bmatrix}[I]\\ [S]\end{bmatrix}. \tag{3}$$

This equation can be generalized to many coupled first-order reactions according to

$$\frac{\mathrm{d}}{\mathrm{d}t}A = K\,A, \tag{4}$$

where A is a vector of concentrations and with the elements of the kinetic matrix K defined as

$$\begin{aligned}K_{jr} &= k_{rj}, r \neq j,\\ K_{jj} &= -\sum_{r\neq j} k_{jr}.\end{aligned} \tag{5}$$

The formal solution to Equation (4) is

$$A(t) = \exp[K\,t]\,A(0). \tag{6}$$

It is possible to handle higher order chemical reactions by defining pseudo first-order rate constants (Cavanagh et al., 1996; Ernst et al., 1987). These are calculated by dividing the reaction rates with the concentration of the reactant molecule. In the case of non-equilibrium reactions these pseudo first-order rate constants are time dependent making the kinetic matrix K time dependent. However, if the system is in chemical equilibrium the kinetic matrix becomes time independent and equivalence with true first-order kinetics is obtained (Cavanagh et al., 1996; Ernst et al., 1987).

The Bloch equations

The Bloch equations in the rotating frame can be used to describe the behavior of the magnetization of spins involved in the chemical exchange if the effect of scalar coupling is ignored. The inhomogeneous Bloch equations (Bloch, 1946) in matrix form are

$$\frac{\mathrm{d}}{\mathrm{d}t}\begin{bmatrix}M_x\\ M_y\\ M_z\end{bmatrix} = -\begin{bmatrix}\lambda & \Omega & -\omega_y\\ -\Omega & \lambda & \omega_x\\ \omega_y & -\omega_x & \rho\end{bmatrix}\begin{bmatrix}M_x\\ M_y\\ M_z\end{bmatrix} + \begin{bmatrix}0\\ 0\\ \rho M_0\end{bmatrix} \tag{7}$$

with

$$\begin{aligned}\omega_x &= -\gamma\,B_1^r cos(\phi),\\ \omega_y &= -\gamma\,B_1^r sin(\phi)\end{aligned} \tag{8}$$

$$\Omega = \omega_0 - \omega_{RF},$$

where Ω is the resonance offset frequency and ω_0 is the Larmor frequency in rad s^{-1}, B_1^r, ω_{RF} and ϕ are the strength, frequency and phase of the applied RF field, respectively, γ is the magnetogyric ratio, ω_x and ω_y are the RF magnetic field components along the x and y axes in rad s^{-1}, respectively, λ is the relaxation rate of transverse magnetization, ρ is the relaxation rate of longitudinal magnetization and M_0 is the equilibrium magnetization.

The Bloch equations can be rewritten in a homogeneous form by appending a constant to the magnetization vector and by including the vector corresponding to correction for equilibrium magnetization into the matrix of coefficients according to

$$\frac{\mathrm{d}}{\mathrm{d}t}\begin{bmatrix}E/2\\ M_x\\ M_y\\ M_z\end{bmatrix} = -\begin{bmatrix}0 & 0 & 0 & 0\\ 0 & \lambda & \Omega & -\omega_y\\ 0 & -\Omega & \lambda & \omega_x\\ -2\rho M_0 & \omega_y & -\omega_x & \rho\end{bmatrix}\begin{bmatrix}E/2\\ M_x\\ M_y\\ M_z\end{bmatrix}, \tag{9}$$

where E stands for unity. The constant with which we extend the magnetization vector was chosen to be *E/2* and not E in order to use the same normalization as used in the product operator formalism (Sørensen et al., 1983). The factor -2 for ρM_0 is due to the minus sign in front of the matrix and the fact that we use *E/2* in the magnetization vector and not E.

McConnell equations

A product space between chemical configuration space and magnetization (Liouville) space is required in order to account for the flow of magnetization during the chemical exchange (Kühne et al., 1979, Binsch, 1969, Jeener, 1982). The product space is created by a direct product of the chemical configura-

tion space vector and the magnetization space vector according to

$$\begin{bmatrix} [I] \\ [S] \end{bmatrix} \otimes \begin{bmatrix} M_x \\ M_y \\ M_z \end{bmatrix} = \begin{bmatrix} I_x \\ I_y \\ I_z \\ S_x \\ S_y \\ S_z \end{bmatrix}. \tag{10}$$

A new kinetics matrix is formed by a direct product between the original kinetic matrix in Equation 3 and a unity matrix of the same size as the magnetization space,

$$\begin{bmatrix} -k_{IS} & k_{SI} \\ k_{IS} & -k_{SI} \end{bmatrix} \otimes \begin{bmatrix} 1 & 0 & 0 \\ 0 & 1 & 0 \\ 0 & 0 & 1 \end{bmatrix} = \begin{bmatrix} -k_{IS} & 0 & 0 & k_{SI} & 0 & 0 \\ 0 & -k_{IS} & 0 & 0 & k_{SI} & 0 \\ 0 & 0 & -k_{IS} & 0 & 0 & k_{SI} \\ k_{IS} & 0 & 0 & -k_{SI} & 0 & 0 \\ 0 & k_{IS} & 0 & 0 & -k_{SI} & 0 \\ 0 & 0 & k_{IS} & 0 & 0 & -k_{SI} \end{bmatrix}. \tag{11}$$

The theoretical basis for the direct product is the sudden jump approximation, which implies that the magnetization does not change orientation during the chemical exchange (Jeener, 1982). The chemical exchange should also be a Markovian random process (Jeener, 1982). The differential equation for the chemical exchange of the spin system can thus be written as

$$\frac{\mathrm{d}}{\mathrm{d}t} \begin{bmatrix} I_{x,chem} \\ I_{y,chem} \\ I_{z,chem} \\ S_{x,chem} \\ S_{y,chem} \\ S_{z,chem} \end{bmatrix} = \begin{bmatrix} -k_{IS} & 0 & 0 & k_{SI} & 0 & 0 \\ 0 & -k_{IS} & 0 & 0 & k_{SI} & 0 \\ 0 & 0 & -k_{IS} & 0 & 0 & k_{SI} \\ k_{IS} & 0 & 0 & -k_{SI} & 0 & 0 \\ 0 & k_{IS} & 0 & 0 & -k_{SI} & 0 \\ 0 & 0 & k_{IS} & 0 & 0 & -k_{SI} \end{bmatrix} \begin{bmatrix} I_{x,chem} \\ I_{y,chem} \\ I_{z,chem} \\ S_{x,chem} \\ S_{y,chem} \\ S_{z,chem} \end{bmatrix}. \tag{12}$$

The matrix for the inhomogeneous Bloch equations must also be expanded to the appropriate product space. This is performed with a direct product between the matrix in Equation 7 and a unity matrix of the same size as the chemical configuration space according to

$$\begin{bmatrix} 1 & 0 \\ 0 & 1 \end{bmatrix} \otimes - \begin{bmatrix} \lambda & \Omega & -\omega_y \\ -\Omega & \lambda & \omega_x \\ \omega_y & -\omega_x & \rho \end{bmatrix} = - \begin{bmatrix} \lambda_I & \Omega_I & -\omega_y & 0 & 0 & 0 \\ -\Omega_I & \lambda_I & \omega_x & 0 & 0 & 0 \\ \omega_y & -\omega_x & \rho_I & 0 & 0 & 0 \\ 0 & 0 & 0 & \lambda_S & \Omega_S & -\omega_y \\ 0 & 0 & 0 & -\Omega_S & \lambda_S & \omega_x \\ 0 & 0 & 0 & \omega_y & -\omega_x & \rho_S \end{bmatrix}. \tag{13}$$

The Bloch equations for the two spins are thus

$$\frac{\mathrm{d}}{\mathrm{d}t} \begin{bmatrix} I_{x,NMR} \\ I_{y,NMR} \\ I_{z,NMR} \\ S_{x,NMR} \\ S_{y,NMR} \\ S_{z,NMR} \end{bmatrix} = - \begin{bmatrix} \lambda_I & \Omega_I & -\omega_y & 0 & 0 & 0 \\ -\Omega_I & \lambda_I & \omega_x & 0 & 0 & 0 \\ \omega_y & -\omega_x & \rho_I & 0 & 0 & 0 \\ 0 & 0 & 0 & \lambda_S & \Omega_S & -\omega_y \\ 0 & 0 & 0 & -\Omega_S & \lambda_S & \omega_x \\ 0 & 0 & 0 & \omega_y & -\omega_x & \rho_S \end{bmatrix} \begin{bmatrix} I_{x,NMR} \\ I_{y,NMR} \\ I_{z,NMR} \\ S_{x,NMR} \\ S_{y,NMR} \\ S_{z,NMR} \end{bmatrix} + \begin{bmatrix} 0 \\ 0 \\ \Theta_I \\ 0 \\ 0 \\ \Theta_S \end{bmatrix}, \tag{14}$$

where Θ_I and Θ_S will be described in the next section.

The McConnell equations are the sum of the chemical exchange contribution described by Equation 12 and the Bloch equations from Equation 14 with $I_x = I_{x,chem} + I_{x,NMR}$, etc, according to

$$\frac{\mathrm{d}}{\mathrm{d}t}\begin{bmatrix} I_x \\ I_y \\ I_z \\ S_x \\ S_y \\ S_z \end{bmatrix} =$$

$$-\begin{bmatrix} \lambda_I + k_{IS} & \Omega_I & -\omega_y & -k_{SI} & 0 & 0 \\ -\Omega_I & \lambda_I + k_{IS} & \omega_x & 0 & -k_{SI} & 0 \\ \omega_y & -\omega_x & \rho_I + k_{IS} & 0 & 0 & -k_{SI} \\ -k_{IS} & 0 & 0 & \lambda_S + k_{SI} & \Omega_S & -\omega_y \\ 0 & -k_{IS} & 0 & -\Omega_S & \lambda_S + k_{SI} & \omega_x \\ 0 & 0 & -k_{IS} & \omega_y & -\omega_x & \rho_S + k_{SI} \end{bmatrix} \quad (15)$$

$$\times \begin{bmatrix} I_x \\ I_y \\ I_z \\ S_x \\ S_y \\ S_z \end{bmatrix} + \begin{bmatrix} 0 \\ 0 \\ \Theta_I \\ 0 \\ 0 \\ \Theta_S \end{bmatrix},$$

with

$$\Theta_I = \rho_I M_{I0}(t), \quad (16)$$

$$\Theta_S = \rho_S M_{S0}(t), \quad (17)$$

$$M_{I0}(t) = M_0 \frac{[I](t)}{[I](t) + [S](t)}, \quad (18)$$

$$M_{S0}(t) = M_0 \frac{[S](t)}{[I](t) + [S](t)}. \quad (19)$$

The equations for calculating the equilibrium magnetization, Equations 18 and 19, can be generalized for N reactants by dividing each reactant concentration with the sum of reactant concentrations using (Ernst et al., 1987; Cavanagh et al., 1996)

$$M_{i0}(t) = M_0 \frac{[A_i](t)}{\sum_j [A_j(t)]}. \quad (20)$$

It should be noted that the equilibrium magnetization described by M_{I0} and M_{S0} are functions of time if the system is not in chemical equilibrium. The McConnell equations can be rewritten in a homogeneous form in the same way as the Bloch equations (Equation 9), if chemical equilibrium is assumed. This is performed by appending a constant term to the product space vector and after that including the vector corresponding to equilibrium magnetization into the matrix of coefficients as the first column according to

$$\frac{\mathrm{d}}{\mathrm{d}t}\begin{bmatrix} E/2 \\ I_x \\ I_y \\ I_z \\ S_x \\ S_y \\ S_z \end{bmatrix} =$$

$$-\begin{bmatrix} 0 & 0 & 0 & 0 & 0 & 0 & 0 \\ 0 & \lambda_I + k_{IS} & \Omega_I & -\omega_y & -k_{SI} & 0 & 0 \\ 0 & -\Omega_I & \lambda_I + k_{IS} & \omega_x & 0 & -k_{SI} & 0 \\ -2\Theta_I & \omega_y & -\omega_x & \rho_I + k_{IS} & 0 & 0 & -k_{SI} \\ 0 & -k_{IS} & 0 & 0 & \lambda_S + k_{SI} & \Omega_S & -\omega_y \\ 0 & 0 & -k_{IS} & 0 & -\Omega_S & \lambda_S + k_{SI} & \omega_x \\ -2\Theta_s & 0 & 0 & -k_{IS} & \omega_y & -\omega_x & \rho_S + k_{SI} \end{bmatrix} \quad (21)$$

$$\times \begin{bmatrix} E/2 \\ I_x \\ I_y \\ I_z \\ S_x \\ S_y \\ S_z \end{bmatrix}.$$

Again, the factor -2 for Θ_I and Θ_S is due to the minus sign in front of the matrix and the fact that we use *E/2* in the product space vector and not *E*.

It is also possible to solve the equations for non-equilibrium reactions by extending the product space with the time dependent equilibrium magnetization calculated using the kinetic matrix according to

$$\frac{\mathrm{d}}{\mathrm{d}t}\begin{bmatrix} M_{I0} \\ M_{S0} \\ I_x \\ I_y \\ I_z \\ S_x \\ S_y \\ S_z \end{bmatrix} =$$

$$-\begin{bmatrix} k_{IS} & -k_{SI} & 0 & 0 & 0 & 0 & 0 & 0 \\ -k_{IS} & k_{SI} & 0 & 0 & 0 & 0 & 0 & 0 \\ 0 & 0 & \lambda_I + k_{IS} & \Omega_I & -\omega_y & -k_{SI} & 0 & 0 \\ 0 & 0 & -\Omega_I & \lambda_I + k_{IS} & \omega_x & 0 & -k_{SI} & 0 \\ -\rho_I & 0 & \omega_y & -\omega_x & \rho_I + k_{IS} & 0 & 0 & -k_{SI} \\ 0 & 0 & -k_{IS} & 0 & 0 & \lambda_S + k_{SI} & \Omega_S & -\omega_y \\ 0 & 0 & 0 & -k_{IS} & 0 & -\Omega_S & \lambda_S + k_{SI} & \omega_x \\ 0 & -\rho_S & 0 & 0 & -k_{IS} & \omega_y & -\omega_x & \rho_S + k_{SI} \end{bmatrix} \quad (22)$$

$$\times \begin{bmatrix} M_{I0} \\ M_{S0} \\ I_x \\ I_y \\ I_z \\ S_x \\ S_y \\ S_z \end{bmatrix}.$$

The equilibrium magnetization as a function of time, M_{I0}(t) and M_{S0}(t), is calculated with help of a copy of the kinetics matrix from Equation 3. This kinetics matrix is put into the upper left corner of the matrix in Equation 15 and the result is Equation 22. The equilibrium magnetization calculated as a function of time in the first two rows of the matrix is fed

into the product space part of the matrix by constants in the first two columns, $-\rho_I$ and $-\rho_S$. The limitation of this equation system is that only first-order kinetics can be considered.

Quantum mechanics

A system of equations describing a quantum mechanical two-spin system during chemical exchange can be obtained using the same method as described previously for classical mechanics. The Bloch equations for *x, y* and *z*-magnetization are replaced by the quantum mechanical master equation in the basis of the Cartesian product operators. This is necessary for a complete description of the behavior of two scalar coupled spin $\frac{1}{2}$ nuclei during pulse sequences. The complete quantum mechanical master equation in the basis of Cartesian product operators has previously been presented both for homonuclear (Allard et al., 1997) and heteronuclear (Allard et al., 1998) two-spin systems. The heteronuclear master equation is published here in a slightly modified form useful for simulations of TROSY (Pervushin et al., 1997) type of experiments. The heteronuclear spin system is assumed to be relaxed by mutual dipole-dipole interaction as well as chemical shift anisotropy interaction with the external magnetic field. Cross-correlation between dipole-dipole (DD) and chemical shift anisotropy (CSA) relaxation is also considered. It should be noted that in the quantum mechanical equations *I* and *S* no longer denote two states in chemical exchange but instead denote two nuclei scalar coupled to each other. The homogenous equation is

$$\frac{\mathrm{d}}{\mathrm{d}t}\begin{bmatrix}
E/2 & 0 & 0 & 0 & 0 & 0 & 0 & 0 & 0 & 0 & 0 & 0 & 0 & 0 & 0 & 0 \\
I_x & 0 & \lambda_I & -\Omega_I & 0 & 0 & 0 & 0 & 0 & 0 & 0 & 0 & 0 & 0 & 0 & 0 \\
I_y & 0 & -\Omega_I & \lambda_I & 0 & 0 & 0 & 0 & 0 & 0 & 0 & 0 & 0 & 0 & 0 & 0 \\
I_z & 0 & 0 & 0 & \rho_I & \omega_{IX} & -\omega_{IV} & 0 & 0 & 0 & 0 & 0 & 0 & 0 & 0 & \delta_I \\
S_x & 0 & 0 & 0 & \omega_{IX} & \rho_I & 0 & 0 & 0 & 0 & 0 & 0 & 0 & 0 & 0 & 0 \\
S_y & 0 & 0 & 0 & -\omega_{IV} & 0 & \rho_I & \sigma & -\omega_{Sy} & \omega_{Sx} & 0 & 0 & 0 & 0 & 0 & 0 \\
S_z & 0 & 0 & 0 & 0 & 0 & \sigma & \rho_S & 0 & 0 & 0 & 0 & 0 & 0 & 0 & \delta_S \\
2I_xS_z & 0 & 0 & 0 & 0 & 0 & -\omega_{Sy} & 0 & \rho_I^a & -\Omega_I & 0 & 0 & 0 & -\omega_{Sy} & \omega_{Sx} & 0 \\
2I_yS_z & 0 & 0 & 0 & 0 & 0 & \omega_{Sx} & 0 & -\Omega_I & \rho_I^a & 0 & 0 & 0 & \omega_{Sx} & -\omega_{Ix} & 0 \\
2I_zS_x & 0 & 0 & 0 & 0 & 0 & 0 & 0 & 0 & 0 & \rho_S^a & \Omega_S & -\Omega_S & 0 & 0 & \omega_{Sy} \\
2I_zS_y & 0 & 0 & 0 & 0 & 0 & 0 & 0 & 0 & 0 & \Omega_S & \rho_S^a & 0 & 0 & \omega_{Ix} & 0 \\
2I_xS_x & 0 & 0 & 0 & 0 & 0 & 0 & 0 & -\omega_{Sy} & \omega_{Sx} & 0 & 0 & \rho_I^a & -\Omega_I & 0 & 0 \\
2I_xS_y & 0 & 0 & 0 & 0 & 0 & 0 & 0 & \omega_{Sx} & \omega_{Sy} & 0 & 0 & -\Omega_I & \rho_I^a & 0 & 0 \\
2I_yS_x & 0 & 0 & 0 & 0 & 0 & 0 & 0 & 0 & 0 & -\omega_{Iy} & \omega_{Ix} & 0 & 0 & \rho_S^a & \Omega_S \\
2I_yS_y & 0 & 0 & 0 & 0 & 0 & 0 & 0 & 0 & 0 & \omega_{Ix} & \omega_{Iy} & 0 & 0 & \Omega_S & \rho_S^a \\
2I_zS_z & 0 & 0 & 0 & 0 & 0 & 0 & 0 & 0 & 0 & 0 & 0 & 0 & 0 & 0 & -2\Theta_{IS}
\end{bmatrix}$$

$$=-\begin{bmatrix}
E/2 & I_x & I_y & I_z & S_x & S_y & S_z & 2I_xS_z & 2I_yS_z & 2I_zS_x & 2I_zS_y & 2I_xS_x & 2I_xS_y & 2I_yS_x & 2I_yS_y & 2I_zS_z \\
0 & 0 & 0 & -2\Theta_I & 0 & 0 & -2\Theta_I & 0 & 0 & 0 & 0 & 0 & 0 & 0 & 0 & 0 \\
0 & 0 & 0 & 0 & 0 & 0 & 0 & \eta_I & \eta_I & \eta_I & \eta_I & 0 & 0 & 0 & 0 & 0 \\
0 & \lambda_I & -\Omega_I & 0 & 0 & 0 & 0 & -\pi J & \pi J & \pi J & -\pi J & 0 & 0 & 0 & 0 & 0 \\
0 & -\Omega_I & \lambda_I & 0 & 0 & 0 & 0 & 0 & 0 & 0 & 0 & 0 & 0 & 0 & 0 & 0 \\
0 & 0 & 0 & \omega_{IV} & -\omega_{IX} & 0 & 0 & 0 & 0 & 0 & 0 & 0 & 0 & 0 & 0 & \delta_I \\
0 & 0 & 0 & \omega_{IX} & \rho_I & 0 & 0 & 0 & 0 & 0 & 0 & 0 & 0 & 0 & 0 & 0 \\
0 & 0 & 0 & -\omega_{IV} & 0 & \rho_I & \sigma & 0 & 0 & 0 & 0 & 0 & 0 & 0 & 0 & \delta_S \\
0 & 0 & 0 & 0 & 0 & \sigma & \rho_S & 0 & 0 & 0 & 0 & 0 & 0 & 0 & 0 & 0 \\
0 & 0 & 0 & 0 & \Omega_S & \lambda_S & -\omega_{Sx} & 0 & 0 & 0 & 0 & 0 & 0 & 0 & 0 & 0 \\
0 & 0 & 0 & 0 & \lambda_S & -\Omega_S & \omega_{Sy} & 0 & 0 & 0 & 0 & 0 & 0 & 0 & 0 & 0 \\
0 & 0 & 0 & 0 & 0 & 0 & 0 & \eta_S & \eta_S & \pi J & -\pi J & 0 & 0 & 0 & 0 & 0 \\
0 & 0 & 0 & 0 & 0 & 0 & 0 & 0 & 0 & 0 & 0 & 0 & 0 & 0 & 0 & 0 \\
0 & 0 & 0 & 0 & 0 & 0 & 0 & 0 & 0 & 0 & 0 & 0 & 0 & 0 & 0 & -2\Theta_{IS}
\end{bmatrix}\begin{bmatrix}
E/2 \\ I_x \\ I_y \\ I_z \\ S_x \\ S_y \\ S_z \\ 2I_xS_z \\ 2I_yS_z \\ 2I_zS_x \\ 2I_zS_y \\ 2I_xS_x \\ 2I_xS_y \\ 2I_yS_x \\ 2I_yS_y \\ 2I_zS_z
\end{bmatrix} \qquad (23)$$

where I and S label ^{1}H and ^{15}N, respectively; Ω_I and Ω_S are the chemical shift offset frequencies in rad s^{-1}; J is the scalar coupling constant in Hz; and ω_{Ix}, ω_{Sx}, ω_{Iy} and ω_{Sy} are the RF magnetic field components at the two frequencies along the x and y axes in rad s^{-1}.

The relaxation rates are

$$\begin{aligned}\lambda_S &= \tfrac{1}{36}A_d^2[2J(0)+\tfrac{3}{2}J(\omega_S)+\tfrac{1}{2}J(\omega_I-\omega_S)\,rr \\ &\quad +3J(\omega_I)+3J(\omega_I+\omega_S)] \\ &\quad +\tfrac{1}{3}A_{cS}^2[\tfrac{2}{3}J(0)+\tfrac{1}{2}J(\omega_S)],\end{aligned} \tag{24}$$

$$\begin{aligned}\lambda_I &= \tfrac{1}{36}A_d^2[2J(0)+3J(\omega_S)+\tfrac{1}{2}J(\omega_I-\omega_S) \\ &\quad +\tfrac{3}{2}J(\omega_I)+3J(\omega_I+\omega_S)] \\ &\quad +\tfrac{1}{3}A_{cI}^2[\tfrac{2}{3}J(0)+\tfrac{1}{2}J(\omega_I)]\end{aligned} \tag{25}$$

$$\begin{aligned}\rho_S &= \tfrac{1}{36}A_d^2[3J(\omega_S)+J(\omega_I-\omega_S) \\ &\quad +6J(\omega_I+\omega_S)]+\tfrac{1}{3}A_{cS}^2[J(\omega_S)],\end{aligned} \tag{26}$$

$$\begin{aligned}\rho_I &= \tfrac{1}{36}A_d^2[J(\omega_I-\omega_S)+3J(\omega_I) \\ &\quad +6J(\omega_I+\omega_S)]+\tfrac{1}{3}A_{cI}^2[J(\omega_I)],\end{aligned} \tag{27}$$

$$\begin{aligned}\rho_S^a &= \tfrac{1}{36}A_d^2[2J(0)+\tfrac{3}{2}J(\omega_S)+\tfrac{1}{2}J(\omega_I-\omega_S) \\ &\quad +3J(\omega_I+\omega_S)]+\tfrac{1}{3}A_{cI}^2[J(\omega_I)] \\ &\quad +\tfrac{1}{3}A_{cS}^2[\tfrac{2}{3}J(0)+\tfrac{1}{2}J(\omega_S)]\end{aligned} \tag{28}$$

$$\begin{aligned}\rho_I^a &= \tfrac{1}{36}A_d^2[2J(0)+\tfrac{1}{2}J(\omega_I-\omega_S)+\tfrac{3}{2}J(\omega_I) \\ &\quad +3J(\omega_I+\omega_S)]+\tfrac{1}{3}A_{cS}^2[J(\omega_S)] \\ &\quad +\tfrac{1}{3}A_{cI}^2[\tfrac{2}{3}J(0)+\tfrac{1}{2}J(\omega_I)],\end{aligned} \tag{29}$$

$$\begin{aligned}\lambda^{mq} &= \tfrac{1}{36}A_d^2[\tfrac{3}{2}J(\omega_S)+\tfrac{1}{2}J(\omega_I-\omega_S) \\ &\quad +\tfrac{3}{2}J(\omega_I)+3J(\omega_I+\omega_S)] \\ &\quad +\tfrac{1}{3}A_{cS}^2[\tfrac{2}{3}J(0)+\tfrac{1}{2}J(\omega_S)] \\ &\quad +\tfrac{1}{3}A_{cI}^2[\tfrac{2}{3}J(0)+\tfrac{1}{2}J(\omega_I)],\end{aligned} \tag{30}$$

$$\begin{aligned}\rho_{IS}^{2sp} &= \tfrac{1}{36}A_d^2[3J(\omega_S)+3J(\omega_I)] \\ &\quad +\tfrac{1}{3}A_{cS}^2[J(\omega_S)]+\tfrac{1}{3}A_{cI}^2[J(\omega_I)],\end{aligned} \tag{31}$$

$$\sigma = \tfrac{1}{36}A_d^2[-J(\omega_I-\omega_S)+6J(\omega_I+\omega_S)], \tag{32}$$

$$\begin{aligned}\mu^{mq} &= \tfrac{1}{36}A_d^2[-\tfrac{1}{2}J(\omega_I-\omega_S) \\ &\quad +3J(\omega_I+\omega_S)],\end{aligned} \tag{33}$$

$$\delta_S = \tfrac{1}{3}A_dA_{cS}\tfrac{1}{2}[3\cos^2(\varphi_S)-1][J(\omega_S)], \tag{34}$$

$$\delta_I = \tfrac{1}{3}A_dA_{cI}\tfrac{1}{2}[3\cos^2(\varphi_I)-1][J(\omega_I)], \tag{35}$$

$$\begin{aligned}\eta_S &= \tfrac{1}{3}A_dA_{cS}\tfrac{1}{2}[3\cos^2(\varphi_S)-1][\tfrac{2}{3}J(0) \\ &\quad +\tfrac{1}{2}J(\omega_S)],\end{aligned} \tag{36}$$

$$\begin{aligned}\eta_I &= \tfrac{1}{3}A_dA_{cI}\tfrac{1}{2}[3\cos^2(\varphi_I)-1][\tfrac{2}{3}J(0) \\ &\quad +\tfrac{1}{2}J(\omega_I)],\end{aligned} \tag{37}$$

with

$$\Theta_I = \rho_I M_{I0} + \sigma M_{S0}, \tag{38}$$

$$\Theta_S = \sigma M_{I0} + \rho_S M_{S0}, \tag{39}$$

$$\Theta_{IS} = \delta_S M_{S0} + \delta_I M_{I0}, \tag{40}$$

where M_{I0} and M_{S0} are the equilibrium magnetizations of ^{1}H and ^{15}N, respectively; λ is the relaxation rate of transverse in-phase magnetization; ρ is the relaxation rate of longitudinal magnetization; ρ_I^a is the relaxation rate of transverse spin I magnetization that is antiphase with respect to spin S; λ^{mq} represent relaxation rates of multiple-quantum coherences; ρ^{2sp} is the relaxation rate of longitudinal two-spin order; σ is the longitudinal cross-relaxation rate; μ^{mq} is a cross-relaxation rate between multiple-quantum coherence components; δ is the longitudinal cross-correlation relaxation rate and η is the transverse cross-correlation relaxation rate; $J(\omega)$ is the spectral density at the angular frequency ω and φ is the angle between the unique axis of the CSA tensor and the internuclear vector r_{IS}.

The spectral densities, $J(\omega)$, are in principle different for the different relaxation mechanisms, but are here considered to be the same. This is a good approximation if φ is small (Tjandra et al., 1996). A useful model for spectral densities is the Lipari-Szabo approach (Lipari and Szabo, 1982a,b), which describe the molecular dynamics using a rotational correlation time τ_m, a correlation time of internal motions τ_e and an order parameter S.

The interaction constants of the CSA and the DD relaxation mechanisms are given by

$$A_{cS} = -\left(\sigma_{S||}-\sigma_{S\perp}\right)\gamma_S B_0, \tag{41}$$

$$A_{cI} = -\left(\sigma_{I||}-\sigma_{I\perp}\right)\gamma_I B_0 \tag{42}$$

and

$$A_d = 3\left(\frac{\mu_0}{4\pi}\right)\left(\frac{\hbar\gamma_I\gamma_S}{r_{IS}^3}\right), \tag{43}$$

respectively, where μ_0 is the permeability of vacuum; r_{IS} is the distance between spins I and S; $\sigma_{||}$ and $\sigma_\perp$ are the shielding constants for the parallel and perpendicular directions in an axially symmetric shielding tensor,

respectively; γ is the magnetogyric ratio and B_0 is the static magnetic field strength of the magnet.

The direct products as described by Equations 10, 11 and 13 applied on the quantum mechanical matrix in Equation 23 without the unity operator *E/2*, will in this case produce a basis set of 30 product operators and two 30×30 matrices. A quantum mechanical analogue to the McConnell equations is thus formed when these two matrices are added together. The 30 coupled differential equations are inhomogeneous, but can be rewritten as a system of 31 coupled homogeneous differential equations in analogy with the transformation of Equation 7 into Equation 9.

Simulating pulse sequences and NMR spectra

The solution to

$$\frac{\mathrm{d}}{\mathrm{d}t}\sigma(t) = -P\sigma(t) \tag{44}$$

which is a homogeneous first-order differential equation, is

$$\sigma(t = t_1 + \Delta t) = \exp[-P\Delta t]\,\sigma(t = t_1)\,, \tag{45}$$

where P and σ are the matrix and vector, respectively, in Equations 9, 21, or 22.

The complex magnetization can be calculated at any time by taking the scalar product of the column vector σ with a row vector that has the elements *1* and *i* in case of *x* magnetization and *y* magnetization, respectively. The detection row vector for Equation 21 is thus

$$\begin{bmatrix} 0 & 1 & i & 0 & 1 & i & 0 \end{bmatrix} \tag{46}$$

and the corresponding detection row vector for Equation 22 is

$$\begin{bmatrix} 0 & 0 & 1 & i & 0 & 1 & i & 0 \end{bmatrix}. \tag{47}$$

The column vector which describes the magnetization at the start of the pulse sequence is for Equation 21

$$\begin{bmatrix} 1/2 \\ 0 \\ 0 \\ M_0\dfrac{[I]}{[I]+[S]} \\ 0 \\ 0 \\ M_0\dfrac{[S]}{[I]+[S]} \end{bmatrix} \tag{48}$$

and for Equation 22

$$\begin{bmatrix} M_0\dfrac{[I](t=0)}{[I](t=0)+[S](t=0)} \\ M_0\dfrac{[S](t=0)}{[I](t=0)+[S](t=0)} \\ 0 \\ 0 \\ M_0\dfrac{[I](t=0)}{[I](t=0)+[S](t=0)} \\ 0 \\ 0 \\ M_0\dfrac{[S](t=0)}{[I](t=0)+[S](t=0)} \end{bmatrix}. \tag{49}$$

These vectors are the starting points for all simulations using the homogeneous McConnell equations as described by Equation 21, or the equations for non-equilibrium first-order kinetics, Equation 22.

Simulations

In order to illustrate the classical part of the theory we have simulated three different NMR experiments useful for studies of slow, intermediate and fast chemical exchange, respectively. The system is in chemical equilibrium in all three cases. The saturation transfer method was used for slow chemical exchange (Forsén and Hoffman, 1963). A plot of line-shape as a function of exchange rate was used for intermediate exchange and finally, a $T_{1\rho}$ experiment as a function of RF field strength was used for fast exchange (Deverell et al., 1970).

As an illustration of the use of Equation 22 for non-equilibrium chemical reactions the line-shape as a function of time after mixing of components was calculated for a stopped-flow experiment (Kühne et al., 1979).

The combination of a quantum mechanical description of a heteronuclear two-spin system with chemical exchange was tested by simulating a sensitivity and gradient enhanced two-dimensional ^{15}N-HSQC (Kay et al., 1992) during slow chemical exchange. The quantum mechanical method of simulation was also tested by simulating the transfer efficiency of a two-dimensional heteronuclear cross-polarization based experiment (Ernst et al., 1991, Allard et al., 1998) as a function of both chemical shift difference between the two states in chemical exchange and the exchange rate constants.

All simulations using the homogeneous McConnell equations were performed using Equations

16–19, 21, 45, 46 and 48, except the simulation of a non-equilibrium chemical reaction which was calculated using Equations 16–19, 22, 45, 47 and 49. The quantum mechanical calculations were performed using the 31×31 matrix obtained as described previously.

Saturation transfer

In Figure 1 we show the transfer of magnetization from spin I to spin S during a saturation transfer experiment (Forsén and Hoffman, 1963). Spin I was selectively saturated using a selective Gaussian 270° pulse followed by a weak on-resonance spin-lock. After a variable time, τ, a hard 90° pulse was applied followed by the calculation of the FID. The exact parameters used are described in the figure legend.

The decay of magnetization on spin S due to chemical exchange with spin I is easily observed in Figure 1 and can in the ideal case be described by the following equation (Forsén and Hoffman, 1963),

$$S_z(\tau) = M_{S0}\left(\frac{k_{SI}}{\rho_S + k_{SI}}\exp\left[-\tau\left(\rho_S + k_{SI}\right)\right] + \frac{\rho_S}{\rho_S + k_{SI}}\right). \quad (50)$$

Both the exchange rate constant, k_{SI}, and the longitudinal relaxation rate of spin S, ρ_S, can in principle be calculated from a fit of Equation 50 to the experimental data. The usual approach, however, is to calculate k_{SI} from the ratio of intensities at time zero and infinity, using a separately measured value for ρ_S according to

$$k_{SI} = \rho_S\left(\frac{S_z(\tau = 0)}{S_z(\tau = \infty)} - 1\right). \quad (51)$$

In the present case the exchange rate constant as calculated from the first and last spectrum in Figure 1 and the known ρ_S using Equation 50 becomes 26% too large. This is because the two resonance peaks are so close to each other, only 150 Hz separation, that it is very difficult to selectively saturate one resonance peak without directly affecting the other.

Line-shape analysis

In Figure 2 we show one-dimensional NMR spectra of a resonance undergoing two-site chemical exchange between state I and S as a function of the exchange rate. The exchange rate constants, k_{IS} and k_{SI}, were changed simultaneously keeping the ratio $k_{IS}/k_{SI} = 1$. The experiment consisted of a single 90°pulse followed by the calculation of the FID. All relevant parameters can be found in the figure legend.

At slow exchange two distinct resonance lines can be observed with negligible life time broadening due to chemical exchange. The resonance lines become very broad at coalescence until a single exchange broadened line is observed at fast chemical exchange, as can be seen in Figure 2.

Relaxation in the rotating frame

Fast chemical exchange is most easily quantifiable by the measurement of the $T_{1\rho}$ or T_2 relaxation time as function of RF field strength (Deverell et al., 1970) or repetition rate of refocusing pulses (Bloom et al., 1965). We have chosen the $T_{1\rho}$ experiment to illustrate our simulation method. In Figure 3 a contour map of the average effective relaxation rate of the two spins in exchange between state I and S as a function of both the RF field strength and the chemical exchange rate constant is shown.

The pulse sequence consisted of a hard 90° pulse followed by a spin-locked relaxation delay and the calculation of the FID. The relevant parameters can be found in the figure legend of Figure 3.

The two exchange rate constants were set to the same value, $k_{IS} = k_{SI}$. The exchange rates used in Figure 3 covers both slow and fast chemical exchange and single exponential functions were therefore fitted separately to the decay of I and S magnetization as a function of mixing time τ. The effective average relaxation rate was calculated as the mean of these two relaxation rates.

The maximum intensity in Figure 3 as a function of exchange rate corresponds to the coalescence case in which the effective relaxation rate is very fast. At both faster and slower chemical exchange the effective relaxation rate is slower. It can be noted that the effective relaxation rate is almost independent of RF field strength when the chemical exchange is fast.

A spin-lock experiment is usually performed on the side of the ridge defined as fast exchange but close to coalescence. In an actual experiment the effective relaxation rate is measured as function of RF field strength and a fit to the following equation is performed in order to obtain the correlation time corresponding to the exchange rate (Davis et al., 1994,

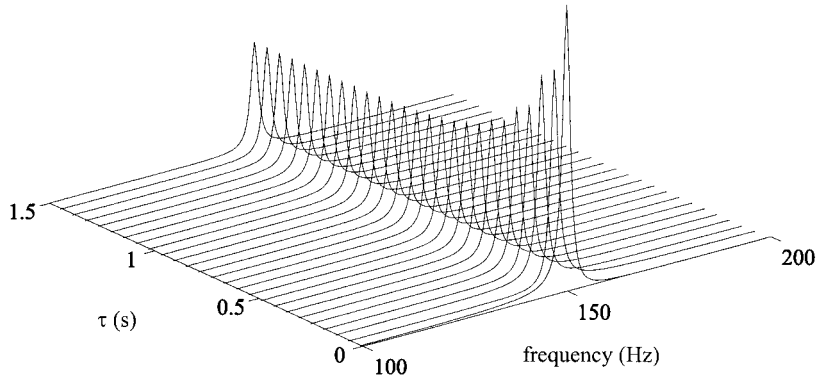

Figure 1. The simulated transfer of saturation from spin I to spin S due to chemical exchange plotted as a function of saturation time, τ. Spin I was selectively saturated by a selective Gaussian 270° pulse followed by an on-resonance spin-lock. After the variable time, τ, a hard 90° pulse was applied followed by the calculation of the FID. The simulation was calculated using Equations 16–19, 21, 45, 46 and 48. The following parameters were used in the simulation. The hard pulse field strength was 25 kHz and the spin-lock field strength was 50 Hz. The 270° Gaussian pulse was 10 ms long and consisted of 512 steps with a maximum field strength of 181 Hz and a truncation level of 1%. The longitudinal relaxation rate of spins I and S were 1 and 1.5 rad s^{-1}, respectively. The transverse relaxation rates were 4 rad s^{-1} for spin I and 5 rad s^{-1} for spin S. The offset resonance frequencies were 0 and 150 Hz for spins I and S, respectively. The exchange rate constants k_{IS} and k_{SI} were both 2 s^{-1}. The FID was calculated as 4000 complex data points with a spectral width of 2000 Hz. No apodization function was used.

Akke and Palmer, 1996):

$$R_{1\rho}^{off} = \rho \cos^2\theta + \lambda \sin^2\theta + (\Omega_I - \Omega_S)^2 \; p_I p_S \frac{\tau_{ex}}{\left(1 + \tau_{ex}^2 \omega_e^2\right)} \sin^2\theta \tag{52}$$

with

$$p_I = \frac{1}{1 + \frac{k_{IS}}{k_{SI}}}, \tag{53}$$

$$p_S = \frac{1}{1 + \frac{k_{SI}}{k_{IS}}}, \tag{54}$$

$$\tau_{ex} = \frac{1}{k_{ex}} = \frac{p_I}{k_{SI}} = \frac{p_S}{k_{IS}}, \tag{55}$$

$$\omega_e = \left(\omega_1^2 + (p_I \Omega_I + p_S \Omega_S)^2\right)^{1/2}, \tag{56}$$

$$\theta = \arctan\left(\frac{\omega_1}{p_I \Omega_I + p_S \Omega_S}\right), \tag{57}$$

$$\omega_1 = -\gamma B_1^r, \tag{58}$$

where ρ and λ are the longitudinal and transverse relaxation rates without contributions from chemical exchange, θ is the tilt angle of the effective field, p_i is the population of spins in site i, ω_1 is the spin-lock field strength in rad s^{-1}, ω_e is the effective field strength in rad s^{-1} and τ_{ex} is the time constant for the exchange process in s^{-1}, which is the inverse of the pseudo first-order rate constant k_{ex}.

In the fit of Equation 52 to the data in Figure 3 the correct time constant for the exchange process was obtained at all exchange rates of 400 Hz and above to within 1%.

Non-equilibrium NMR

In Figure 4 we show a simulated variant of a stopped-flow NMR experiment (Kühne et al., 1979). Only the component in which spin I reside exists at the beginning and the component in which spin S resides appear as a result of chemical exchange. One-dimensional spectra are plotted as a function of the time after mixing. The pulse sequence consisted of mixing of components, a time delay τ, a 90° pulse, and the calculation of the FID. The relevant parameters are described in figure legend 4.

The S magnetization appears with a dispersive line-shape in the first spectra since the concentration of S at the start of the FID is zero. At faster chemical exchange most of the I magnetization would already have appeared after a few points in the FID and the line-shape becomes predominately absorptive (Kühne et al., 1979). The system approaches equilibrium rapidly and the last spectrum has the correct intensity ratio according to the rate constants, see Figure 4.

Quantum mechanical simulations

The quantum mechanical method of simulation was tested by simulating a sensitivity and gradient enhanced two-dimensional ^{15}N-HSQC (Kay et al., 1992) during slow chemical exchange between two states.

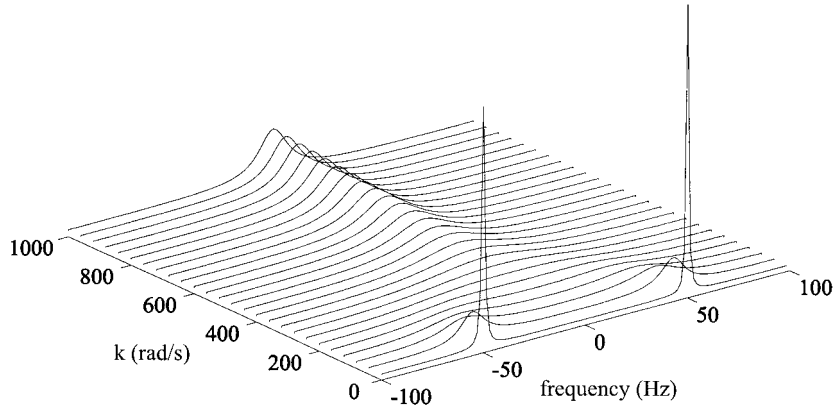

Figure 2. Simulated one-dimensional spectra of spin I and spin S in exchange as a function of exchange rate. The ratio of exchange rate constants, k_{IS} and k_{SI}, was set to 1 in order to keep the equilibrium constant at a constant value. The pulse sequence consisted of a single 90° pulse, directly followed by the calculation of the FID. The simulation was calculated using Equations 16–19, 21, 45, 46 and 48. The hard pulse field strength was 25 kHz. The longitudinal and transverse relaxation rates were 1 and 4 rad s^{-1}, respectively, for spin I and 1.5 and 5 rad s^{-1}, respectively, for spin S. The offset resonance frequency was for spin I equal to −50 Hz and for spin S equal to 50 Hz. The spectral width was 200 Hz and a FID of 128 complex points was calculated. No apodization function was used.

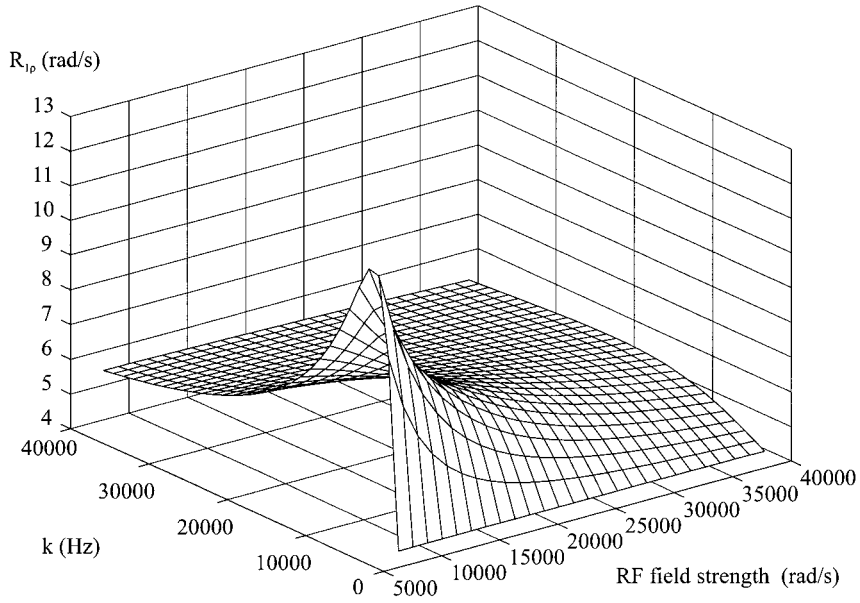

Figure 3. The simulated contour map of the average effective relaxation rate of spin I and S in exchange during a $T_{1\rho}$ experiment plotted as a function of both the RF field strength and the chemical exchange rate. The pulse sequence consisted of a hard 90° pulse followed by a spin-locked relaxation delay and the calculation of the FID. The two exchange rate constants, k_{IS} and k_{SI}, were set to the same value. Single exponential functions were fitted separately to the decay of I and S magnetization. The effective average relaxation rate was calculated as the mean of the relaxation rates of I and S magnetization. The simulation was calculated using Equations 16–19, 21, 45, 46 and 48. The hard pulse field strength was 25 kHz. The longitudinal relaxation rates for spins I and S were 1 and 1.5 rad s^{-1}, respectively. The transverse relaxation rates were 4 rad s^{-1} for spin I and 5 rad s^{-1} for spin S. The offset resonance frequencies were −50 and 50 Hz for spins I and S, respectively. Relaxation delays between 0 and 500 ms in 21 steps were used in the fit of single exponential decays. No apodization function was used.

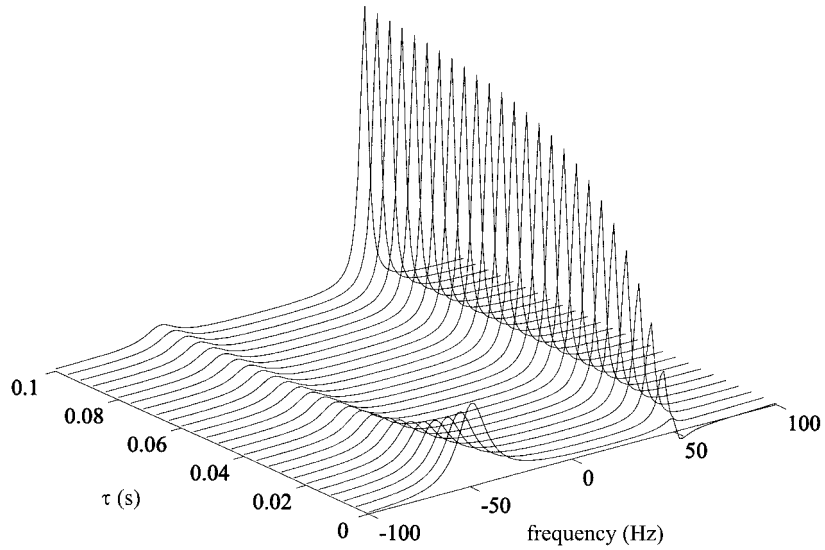

Figure 4. A simulated stopped-flow NMR experiment. The one-dimensional spectra are plotted as a function of time after mixing of components. The pulse sequence consisted of mixing of components followed by a time delay τ, a 90° pulse and the calculation of the FID. Only the component in which spin *I* reside exist from start and the component in which spin *S* reside appear as a result of chemical exchange. The simulation was calculated using Equations 16–19, 22, 45, 47 and 49. The exchange rate constants k_{IS} and k_{SI} were 50 and 10 s^{-1}, respectively. The longitudinal relaxation rate of spins *I* and *S* were 1 and 1.5 rad s^{-1}, respectively. The transverse relaxation rates were 4 rad s^{-1} for spin *I* and 5 rad s^{-1} for spin *S*. The offset resonance frequency was for spin *I* equal to -50 Hz and for spin *S* equal to 50 Hz. A total of 128 complex points were calculated for each FID. The spectral width was 200 Hz. No apodization function was used.

No decoupling was used in either of the two dimensions.

A ^{1}H-^{15}N pair of spins with scalar coupling constant of 92 Hz was considered. The offset chemical shifts were 200 Hz for both proton and nitrogen in one state, which is in exchange with another state with the offset chemical shift of -200 Hz for both proton and nitrogen. The exchange rate constants for the forward and reverse reaction were both set to 10 s^{-1}. All other relevant parameters can be found in figure legend 5.

In the simulated two-dimensional spectra the two states of the spin system each gives rise to four resonance peaks because no decoupling was used in either dimension. The four resonance peaks are of different height due to the line-narrowing effect caused by cross-correlation between DD and CSA relaxation. This is the effect used in TROSY (Pervushin et al., 1997) experiments, in which only the most narrow component of the four is retained. The slow exchange is the reason for the appearance of cross-peaks between the two states. The cross-peaks also consist of four peaks with the same intensity ratio as the auto-peaks.

The quantum mechanical method of simulation was also tested by simulating the transfer efficiency of a two-dimensional heteronuclear cross-polarization based experiment (Ernst et al., 1991; Allard et al., 1998) as a function of both chemical shift difference and exchange rate constants, Figure 6. The chemical shifts of ^{1}H and ^{15}N for the two states were changed simultaneously and with the same value. For a chemical shift difference of 200 Hz the chemical shifts of both ^{1}H and ^{15}N were -100 Hz in the first state and $+100$ Hz in the second state. The two exchange rate constants were set to the same value. Other relevant parameters can be found in figure legends 5 and 6.

The height in Figure 6 is the fraction of magnetization that survives the pulse sequence and is available for detection. No effect of a change in exchange rate constants can be observed when the chemical shift difference frequency is 0 Hz. The opposite is also true, no effect on the transfer efficiency as a function of changes in the chemical shift difference frequency can be observed if the exchange rate is 0 Hz. The location of the valley on the exchange rate scale in Figure 6 is a function of the strength of the DIPSI-2 RF field. Larger chemical shift difference between the two states gives larger losses of magnetization during the pulse sequence, as can be observed in Figure 6.

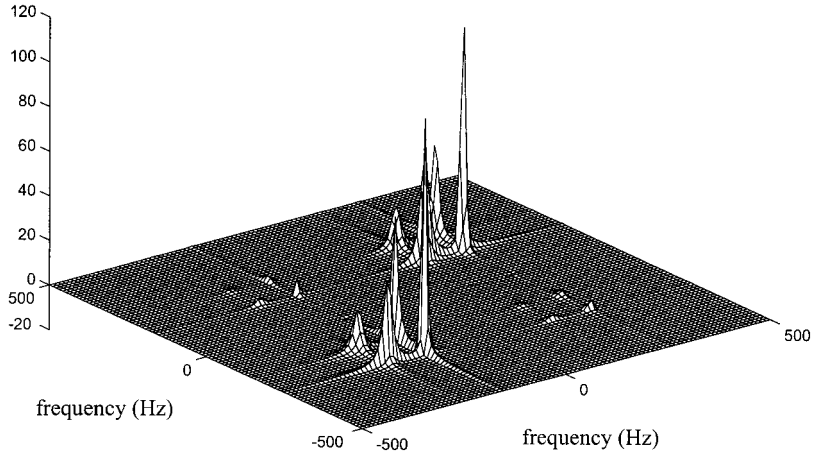

Figure 5. A simulated sensitivity and gradient enhanced two-dimensional ^{15}N-HSQC (Kay et al., 1992) without decoupling in either of the two dimensions. The offset chemical shifts were 200 Hz for both proton and nitrogen in one state, which is in exchange with another state with the offset chemical shift of -200 Hz for both proton and nitrogen. The exchange rate constants for the forward and reverse reaction were both 10 s^{-1}. The ^{1}H and ^{15}N RF field strengths were 50000 Hz and 5555 Hz, respectively. The pulsed field gradients were 2.5 ms and 0.25 ms long and applied with strengths of 30 and 30.4 gauss cm^{-1}, respectively. A total of 16 slices were simulated and added together in order to simulate the pulsed field gradients (Allard et al., 1998). The number of complex data-points simulated were 96 with a dwell time of 0.001 s in both dimensions. A cosine apodization function was used without any zero-filling. A ^{1}H-^{15}N pair of spins with scalar coupling constant of 92 Hz was assumed. A magnetic field strength of 18.8 T was used. The dynamics responsible for relaxation were described by $\tau_m = 25$ ns, $\tau_e = 50$ ps and $S^2 = 0.8$ (Lipari and Szabo, 1982a, b). The proton and the nitrogen was relaxed by mutual DD interactions using $r_{IS} = 1.02$ Å, and by CSA interactions with the external field using $(\sigma_{||} - \sigma_{\perp}) = -14$ ppm and -160 ppm, respectively. The angle between the unique axis of the CSA tensor and the internuclear vector between proton and nitrogen was set to 0° and 22° for the proton and the nitrogen, respectively. No other relaxation mechanisms were considered, which corresponds to a completely deuturated protein.

Discussion

The advantages of rewriting the inhomogeneous differential equations present in NMR into homogeneous differential equations has long been recognized. The homogeneous form of the quantum mechanical master equation in the basis of level shift operators has been presented both with and without chemical exchange (Jeener, 1982; Smith et al., 1994; Cuperlovic et al., 2000). The extended Solomon equations (Canet, 1989) have been solved using the homogeneous master equation in the basis of Cartesian product operators (Levitt and Bari, 1992, 1994). The homogeneous form of the Bloch-Solomon equations has been derived from the complete homogeneous master equation for a homonuclear spin system (Allard et al., 1997) and the complete homogeneous master equation for a heteronuclear spin system in the basis of Cartesian product operators has been presented (Allard et al., 1998).

The major advantage of rewriting inhomogeneous differential equations into homogeneous differential equations is that the solution to a system of homogeneous differential equations is simply the exponent of the matrix of coefficients, Equation 45. The exponent of the matrix is also a matrix. This matrix for a particular time period in a pulse sequence is the (superoperator) propagator for both the magnetization and the chemical exchange. The solution to a complete pulse sequence is the time ordered product of propagators for the individual pulse sequence elements. This product of matrixes is a matrix and it is the effective propagator for the complete pulse sequence. The result of a complete pulse sequence can thus be described by the multiplication of a vector containing the magnetization and concentrations at the start of the pulse sequence, with the matrix corresponding to the effective propagator for the pulse sequence. This allows for time-efficient numerical calculations.

The effective Liouvillian (Allard et al., 1998; Levitt and Bari, 1992, 1994) for a pulse sequence can be calculated by taking the natural logarithm of the effective propagator and dividing it with the total time for the pulse sequence, followed by a change of sign (Allard et al., 1998). The effective Liouvillian is a useful source for target functions in the optimization of pulse sequences. Mixing sequences, decoupling sequences and shaped pulses are examples of pulse sequences that can be optimized.

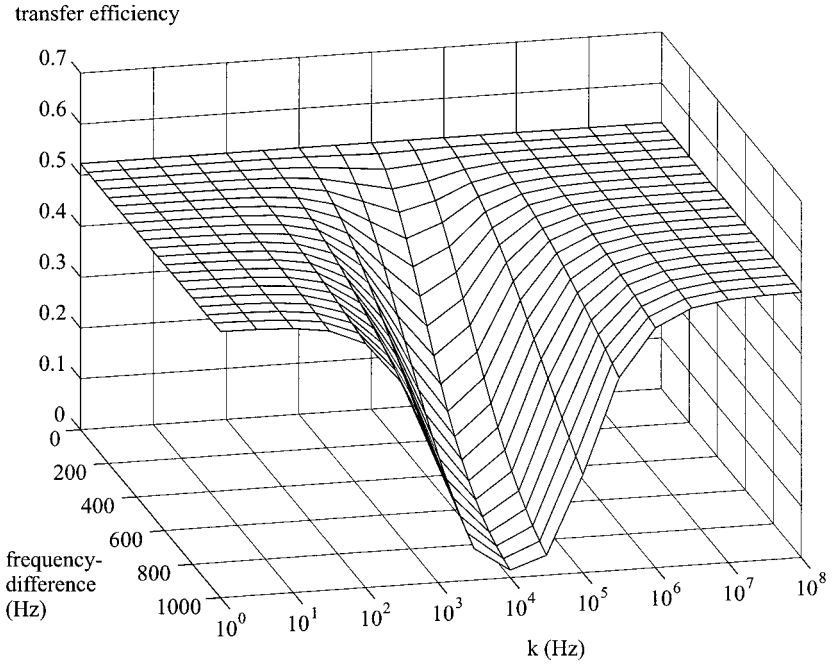

Figure 6. The simulated transfer efficiency of a two-dimensional heteronuclear cross-polarization based experiment (Ernst et al., 1991; Allard et al., 1998) as a function of both chemical shift difference and exchange rate constants. The exchange rate constants for the forward and reverse reaction were set to the same value. The chemical shifts of ^{1}H and ^{15}N for the two states were changed simultaneously and symmetrically around the carrier frequency. This means that for a chemical shift difference of 200 Hz the chemical shifts of both ^{1}H and ^{15}N were -100 Hz in the first state $+100$ Hz and in the second state. The ^{1}H RF field strengths were 50000 Hz and 5555 Hz during hard pulses and DIPSI-2 mixing (Shaka et al., 1988), respectively. The ^{15}N RF field strength was 5555 Hz. The DIPSI-2 mixing times were 10.36 ms, which corresponds to two (R, $\overline{R}$, $\overline{R}$, R) supercycles. All other relevant parameters were the same as in figure legend 5.

Simulations of pulse sequences can be very useful in the analysis of experimental results. Consider, for instance, the case when saturation transfer (Forsén and Hoffman, 1963) is used in order to measure the exchange rate constant between two states that have chemical shifts close to each other. It is then impossible to saturate one resonance peak using an RF field without directly affecting the other. Direct application of Equations 50 or 51 will then fail to provide the correct exchange rate constant. This can be observed in Figure 1 in which the exchange rate, as calculated using Equation 51, becomes 26% too large. If the two resonance peaks were separated with 500 Hz instead of 150 Hz the exchange rate would be within 2% the same as the exchange rate used in the simulation. A complete simulation using the homogeneous McConnel equations with fitting of theoretical spectra to experimental spectra can solve this problem.

An interesting use of the equations for non-equilibrium reactions is in the study of protein folding (Balbach et al., 1995, 1996). One way of performing protein folding experiments is to start acquiring a two-dimensional ^{15}N-HSQC directly after initiating folding (Balbach et al., 1996). Refolding is completed within the accumulation time of the experiment. This experiment can be simulated without approximations using equations in this paper.

Conclusions

We have rewritten the McConnell equations in a homogeneous form in order to facilitate fast and simple simulations of pulse sequences whenever chemical exchange is important. The equation system was tested on pulse sequences useful for the study of slow, intermediate and fast exchange.

We have also presented equations that can simulate pulse sequences during non-equilibrium chemical reactions, as long as the chemical exchange can be described by first-order kinetics.

Finally, a quantum mechanical treatment of a heteronuclear two-spin system in chemical exchange is presented.

We expect these equations to be useful in the analysis of NMR experiments aimed at the study of chemical exchange whenever ideal experimental circumstances can not be provided. The equations should also be useful in the development of new pulse sequence elements aimed at the study of chemical exchange using the effective Liouvillian approach.

Acknowledgements

This work was supported by the Swedish Natural Sciences Research Council and the Sven and Ebba-Christina Hagbergs Foundation.

References

Akke, M. and Palmer, A.G. (1996) *J. Am. Chem. Soc.*, **118**, 911–912.

Allard, P., Helgstrand, M. and Härd, T. (1997) *J. Magn. Reson.*, **129**, 19–29.

Allard, P., Helgstrand, M. and Härd, T. (1998) *J. Magn. Reson.*, **134**, 7–16.

Balbach, J., Forge, V., Lau, W.S., van Nuland, N.A.J., Brew, K. and Dobson, C.M. (1996) *Science*, **274**, 1161–1163.

Balbach, J., Forge, V., van Nuland, N.A.J., Winder, S.L., Hore, P.J. and Dobson, C.M. (1995) *Nature Struct. Biol.*, **2**, 865–870.

Binsch, G. (1969) *J. Am. Chem. Soc.*, **91**, 1304–1309.

Bloch, F. (1946) *Phys. Rev.*, **70**, 460–474.

Bloom, M., Reeves, L.W. and Wells, E.J. (1965) *J. Chem. Phys.*, **42**, 1615–1624.

Canet, D. (1989) *Prog. NMR Spectrosc.*, **21**, 237–291.

Cavanagh, J., Fairbrother, W.J., Palmer, A.G. and Skelton, N.J. (1996) *Protein NMR Spectroscopy: Principles and Practice*, Academic Press, San Diego.

Cuperlovic, M., Meresi, G.H., Palke, W.E. and Gerig, J.T. (2000) *J. Magn. Reson.*, **142**, 11–23.

Davis, D.G., Perlman, M.E. and London, R.E. (1994) *J. Magn. Reson. B*, **104**, 266–275.

Deverell, C., Morgan, R.E. and Strange, J.H. (1970) *Mol. Phys.*, **18**, 553–559.

Ernst, M., Griesinger, C., Ernst, R.R. and Bermel, W. (1991) *Mol. Phys.*, **74**, 219–252.

Ernst, R.R., Bodenhausen, G. and Wokaun, A. (1987) *Principles of Nuclear Magnetic Resonance in One and Two Dimensions*, Oxford University Press, Oxford.

Forsén, S. and Hoffman, R.A. (1963) *Acta Chem. Scand.*, **17**, 1787–1788.

Gutowsky, H.S., McCall, D.W. and Slichter, C.P. (1953) *J. Chem. Phys.*, **21**, 279–292.

Jeener, J. (1982) *Adv. Magn. Reson.*, **10**, 1–51.

Kaplan, J. (1958) *J. Chem. Phys.*, **28**, 278–282.

Kaplan, J.I. and Fraenkel, G. (1980) *NMR of Chemically Exchanging Systems*, Academic Press, New York.

Kay, L.E., Keifer, P. and Saarinen, T. (1992) *J. Am. Chem. Soc.*, **114**, 10663–10665.

Kühne, R.O., Schaffhauser, T., Wokaun, A. and Ernst, R.R. (1979) *J. Magn. Reson.*, **35**, 39–67.

Levitt, M.H. and Bari, L.D. (1992) *Phys. Rev. Lett.*, **69**, 3124–3127.

Levitt, M.H. and Bari, L.D. (1994) *Bull. Magn. Reson.*, **16**, 94–114.

Lipari, G. and Szabo, A. (1982a) *J. Am. Chem. Soc.*, **104**, 4546–4559.

Lipari, G. and Szabo, A. (1982b) *J. Am. Chem. Soc.*, **104**, 4559–4570.

McConnell, H.M. (1958) *J. Chem. Phys.*, **28**, 430–431.

McLaughlin, A.C. and Leigh, J.S. (1973) *J. Magn. Reson.*, **9**, 296–304.

Pervushin, K., Riek, R., Wider, G. and Wüthrich, K. (1997) *Proc. Natl. Acad. Sci. USA*, **94**, 12366–12371.

Shaka, A.J., Lee, C.J. and Pines, A. (1988) *J. Magn. Reson.*, **77**, 274–293.

Smith, S.A., Palke, W.E. and Gerig, J.T. (1994) *J. Magn. Reson. A*, **106**, 57–64.

Sørensen, O.W., Eich, G.W., Levitt, M.H., Bodenhausen, G. and Ernst, R.R. (1983) *Prog. NMR Spectrosc.*, **16**, 163–192.

Tjandra, N., Szabo, A. and Bax, A. (1996) *J. Am. Chem. Soc.*, **118**, 6986–6991.

Wennerström, H. (1972) *Mol. Phys.*, **24**, 69–80.